IJPSR (2017), Vol. 8, Issue 2 (Research Article)

INTERNATIONAL JOURNAL OF PHARMACEUTICAL SCIENCES AND RESEARCH

Received on 06 August, 2016; received in revised form, 26 October, 2016; accepted, 17 November, 2016; published 01 February, 2017

# FRONTIER MOLECULAR, NATURAL BOND ORBITAL, UV-VIS SPECTRAL STUDY, SOLVENT INFLUENCE ON GEOMETRIC PARAMETERS, VIBRATIONAL FREQUENCIES AND SOLVATION ENERGIES OF 8-HYDROXYQUINOLINE

Muhammad Khalid [*1, 2] Muhammad Ali [3], Muhammad Aslam [4], Sajjad Hussain Sumrra [5], Muhammad Usman Khan [6], Nadeem Raza [7], Naresh Kumar [8] and Muhammad Imran [9]

Departamento de Química Fundamental [1], Instituto de Química, Universidade de São Paulo, Av. Prof. Lineu Prestes, 748, São Paulo, 05508-000, Brazil.
Department of Chemistry [2], University of Education Lahore, Faisalabad Campus, Pakistan.
Department of Physics [3], Faculty of Science and Technology, Umeå University, 901 87, Umeå Sweden.
Department of Chemistry [4], University of Education, Lahore, Pakistan.
Department of Chemistry [5], Institute of Natural Sciences, University of Gujrat, Gujrat, Pakistan.
Department of Applied Chemistry and Biochemistry [6], Government College University Faisalabad, Faisalabad, Pakistan.
Institute of Chemical Sciences [7], Bahauddin Zakariya University, Multan, Pakistan.
Department of Chemistry [8], UCG Thar Project, Islamkot, Sindh Pakistan.
Department of Chemistry [9], The University of Azad Jammu & Kashmir Muzaffarabad, AJK, Pakistan.

**Keywords:**

8-Hydroxyquinoline; polarizable continuum model; density-based solvation model; Natural bond orbital; frontier molecular orbitals

**Correspondence to Author:**
**Dr. Muhammad Khalid**

Assistant Professor
Department of Chemistry, University of Education Lahore, Faisalabad Campus, Faisalabad, Pakistan.

**E-mail:** khalid@iq.usp.br

**ABSTRACT:** *N*-heterocyclic compounds have extensive biological and pharmaceutical applications. 8-Hydroxyquinoline (8-HQ) also plays a significant role in many fields of life. The excellent biological significance of the 8-HQ prompted us to extend the DFT based studies. The frontier molecular orbitals (FMOs), UV-VIS and solvation model based studies remained unknown. Therefore, we intended to study the natural bond orbital, FMOs, UV-VIS, thermodynamic properties and medium influence on solvation energies, dipole moment, FT-IR and FT-Raman using polarizable continuum model (PCM) and density-based solvation model (SMD). The electronic properties of molecule were calculated by M06-2X/6-31G (d,P) and B3LYP/6-31G (d,p) level of theories. The solvent influence on the geometric parameters, FT-IR and FT-Raman were studied by B3LYP /6-31G(d) method. A good correspondence is found between the optimized parameters and the reported X-ray data. Natural bond orbital reveals that the maximum stabilization energy reached up to 39.64kJ/mol which is responsible for extra stability of the molecule. In solvated 8-HQ, a significant medium effects on FT-IR and FT-Raman intensities is observed. The intensities enhanced from gas to solvent phase. The solvation free energies are found to be -28.710 and -39.456 kJ/mol in PCM and SMD models respectively. FMOs suggested that this molecule contain less hardness and larger softness values. These findings reveal that the molecule might be bioactive.

**INTRODUCTION:** *N*-heterocyclic compounds are most versatile organic compounds contain broad spectrum biological and pharmaceutical significance.[1]

QUICK RESPONSE CODE

DOI: 10.13040/IJPSR.0975-8232.8(2).457-69

Article can be accessed online on: www.ijpsr.com

DOI link: http://dx.doi.org/10.13040/IJPSR.0975-8232.8 (2).457-69

In this context, 8-hydroxyquinoline (1-azanaphthalene) is also one of the N-heterocyclic compounds which play a fundamental role in many fields of life. The compound 8-hydroxyquinoline (8-HQ) has been used as preservative in textile, wood and paper industries. [2] It is used in the chemicals which help to kill the crop insects and pests in an agricultural field.[1, 2] It is also used as antimalarial, [3] antibacterial, [4] anticancer drugs, [5] anthelmintic, amebicidal, anti-HIV [6] and neuroprotective. [3]

It is used as a powerful chelator for the treatment of diseases caused by metals. [6, 2] A basic component of organic light emitting diode (OLEDs) is Alq3 which is produced by the reaction of 1-azanapthalene and aluminum (III). [4] 8-HQ and its derivatives have multiple applications that range from pharmacological and pharmaceutical agents to carries the electron in OLEDs and fluorescent chemo sensor for metal ions as well as very useful chelating agent in analytical and radioactive chemistry. [2, 7] 8-HQ has strong fluorescence in concentrated acids, water dearth of fluorescence or clusters of hydrogen-bonded with water, alcohol and ammonium molecules.

Due to these outstanding applications, various DFT based studies have been reported on this molecule as; Arıcı *et al.* (2005) have reported IR in gas phase. [8] Krishnakumar *et al.* (2005) also reported FT-IR and FT-Raman spectra in gas phase. [9] R. P. Gangadharan *et al.* (2014) reported NBO using B3LYP with 6-31G (d, p) basis set, [10] however, some discrepancies have been observed regarding the assignment of NBO analysis.

Usually, FT-IR vibrational spectra based on computational analysis is performed in the gas phase as carried out regarding this molecule. [6, 7] However, the experimental studies mostly include in solvent phase. Hence, it is important to consider solvent effects in computational approaches. The chemistry of the molecule under investigation can be changed due to synergic effect of the solvent and the solute. The solvent-solute association can modify stability, energy (i.e. vibrational frequency, spectrum) and molecular arrangement as well as play a vital role in the pharmaceutical industry for drug design.[11]

As In 1890, W. Ostwald wrote:

"Almost all the chemical processes, which occur in nature, whether in animal or vegetable organisms or in non-living surface of the Earth ... take place between substances in solution"

To the best of our knowledge, neither frontier molecular orbitals (FMOs), global reactivity parameters, UV-VIS analysis nor the solvation models based DFT regarding title molecule are reported so for.

Therefore, the objective of our study is to present the frontier molecular orbitals (FMOs), global reactivity parameters, UV-VIS analysis and also to explore the solvent effects on geometry, FT-IR, FT-Raman spectra and solvation energy of title molecule using Polarizable Continuum Model (PCM) and Density-based Solvation Model (SMD). Moreover, one of the main objectives of our study is also to improve the scientific contribution by elucidating the right assignment in NBO analysis using same level of theory as reported [B3LYP/6-31G (d,p)] and more accurate M06-2X/6-31G (d,P) method.

**MATERIALS AND METHODS:** Complete calculations were performed using Gaussian 09 program package [12] with density functional theory (DFT) [13-15] at the M06-2X/6-31G (d,P) and B3LYP/6-31G (d,p)/ 6-31G (d) levels of theory. The geometry optimization and frequency calculations were performed for title compound. Consequently, a nonattendance of negative eigen value demonstrated that the geometry of the compound is in the globle minima of the potential energy surface.

All input files were prepared using Gauss View 5.0.16 Chemcraft, [17] Gauss View 5.0 and Avogadro software [18] were used to analyze the output files.

**RESULTS AND DISCUSSION:** Equilibrium geometry: The 8-HQ geometry is optimized by using M06-2X and B3LYP level of theories with basis set as 6-31G(d,p). However, the molecule is also optimized at B3LYP/6-31G(d) method in gas phase and dimethyl sulfoxide as a solvent to study the solvent influence on optimized geometry. The obtained parameters are tabulated in **Table 1**.

The geometry of a compound is very important to study the vibrational frequencies since slight alteration in geometry can significantly alter the frequency. The intermolecular forces are more essential in this context, when any molecule goes from gaseous to solution phase. Subsequently solute-solvent interactions take place and might be geometry of solute changes.[8] Keeping in view these solute-solvent interactions, we studied our system in gas and solvent phase. **Table 1** shows a variation in bond lengths and angles.

The bond lengths such as R(1-2), R(3-4), R(4-18), R(5-16), R(10-13), R(16-17) are slightly increased in solvent phase than gas phase. However, some bond lengths like that R(1-8), R(2-9), R(4-5), R(6-11), R(7-10), R(12-13) and R(13-15) are slightly decreased in solvent phase as compared to gas phase. These variations are occurred only in third decimal. Interestingly, some bond lengths i.e. R(1-6), R(2-3), R(3-10), R(12-14), R(12-18) are found exactly similar in both phases. Moreover, the obtained bond lengths show good agreement to the X-ray data [19] and DFT based observed bond lengths. [6]

Furthermore, the bond angles like A(1-2-9), A(1-6-11), A(4-3-10), A(3-10-7), A(5-4-18), A(4-5-6), A(5-16-17), A(13-12-18) and A(14-12-18) are slightly increased in solvent phase than gas phase. While an opposite trend is observed in A(1-6-5), A(2-3-4), A(2-3-10), A(3-4-18), A(6-5-16) and A(12-13-15) where bond angles are decreased in solvent phase to a little extent than gas phase. However, bond angles such as A(2-1-6), A(2-1-8), A(1-2-3), A(6-1-8), A(3-2-9), A(3-4-5), A(3-10-13), A(4-5-16), A(4-18-12), A(10-13-12) and A(10-13-15) exhibited exactly similar trend in both phases. Hence, the straightforward relation is not observed between solvent and gas phase.

The found bond angles show correspondence with the X-ray data [11] and DFT based calculated bond angles. [12]

**TABLE 1: COMPARISON OF SELECTED BOND LENGTHS (Å) AND ANGLES (°) FOR 8-HQ.**

| Bond length | Gas Phase | Solvent Phase[a] | Bond Angle | Gas Phase | Solvent Phase[a] |
|---|---|---|---|---|---|
| R(1-2) | 1.375 | 1.377 | A(2-1-6) | 120.9 | 120.9 |
| R(1-6) | 1.414 | 1.414 | A(2-1-8) | 120.3 | 120.3 |
| R(1-8) | 1.087 | 1.086 | A(1-2-3) | 119.7 | 119.7 |
| R(2-3) | 1.42 | 1.42 | A(1-2-9) | 121 | 121.1 |
| R(2-9) | 1.087 | 1.086 | A(6-1-8) | 118.8 | 118.8 |
| R(3-4) | 1.431 | 1.432 | A(1-6-5) | 120.9 | 120.7 |
| R(3-10) | 1.42 | 1.42 | A(1-6-11) | 119.6 | 119.7 |
| R(4-5) | 1.434 | 1.433 | A(3-2-9) | 119.3 | 119.3 |
| R(4-18) | 1.361 | 1.364 | A(2-3-4) | 120.3 | 120.2 |
| R(5-6) | 1.383 | 1.383 | A(2-3-10) | 122.9 | 122.8 |
| R(5-16) | 1.358 | 1.362 | A(4-3-10) | 116.8 | 117 |
| R(6-11) | 1.089 | 1.088 | A(3-4-5) | 118.4 | 118.4 |
| R(7-10) | 1.088 | 1.087 | A(3-4-18) | 123 | 122.8 |
| R(10-13) | 1.374 | 1.375 | A(3-10-7) | 119.1 | 119.2 |
| R(12-13) | 1.418 | 1.416 | A(3-10-13) | 119.7 | 119.7 |
| R(12-14) | 1.09 | 1.09 | A(5-4-18) | 118.6 | 118.8 |
| R(12-18) | 1.32 | 1.32 | A(4-5-6) | 119.9 | 120 |
| R(13-15) | 1.086 | 1.085 | A(4-5-16) | 116.9 | 116.9 |
| R(16-17) | 0.971 | 0.972 | A(4-18-12) | 117.8 | 117.8 |

B3LYP /6-31G(d), [a]solvent=DMSO

**TABLE 1: Continued.....**

| Bond Angle | Gas Phase | Solvent Phase[a] |
|---|---|---|
| A(6-5-16) | 123.2 | 123 |
| A(5-6-11) | 119.5 | 119.6 |
| A(5-16-17) | 108.4 | 108.7 |
| A(7-10-13) | 121.2 | 121.1 |
| A(10-13-12) | 118.6 | 118.6 |
| A(10-13-15) | 121.5 | 121.5 |
| A(13-12-14) | 119.6 | 119.5 |
| A(13-12-18) | 124.1 | 124.2 |
| A(12-13-15) | 120 | 119.9 |
| A(14-12-18) | 116.3 | 116.4 |

**Natural Bond Orbital (NBO) Analysis:** The natural bond orbital (NBO) analysis is a proficient method to study the intra- and inter-molecular bonding, the charge transfer and conjugative interaction between the electron donor and acceptor. [9, 2] In the presence of large stabilization energy electron donors have more rigorous interactions with electron acceptors. NBO analysis is useful to transmit of electron density form filled electron orbital to unoccupied orbital. [20] According to second order perturbation approach, the stabilization energy formula can be shown by Equations 1.

$$E^{(2)} = q_i \frac{(F_{i,j})^2}{\varepsilon_j - \varepsilon_i} \qquad \text{Equations 1}$$

Where $E^{(2)}$ is stabilization energy, $q_i$ donor orbital occupancy, $F(i.j)$ is the diagonal and $\varepsilon_j$ and $\varepsilon_i$ are the off-diagonal NBO Fock matrix elements.

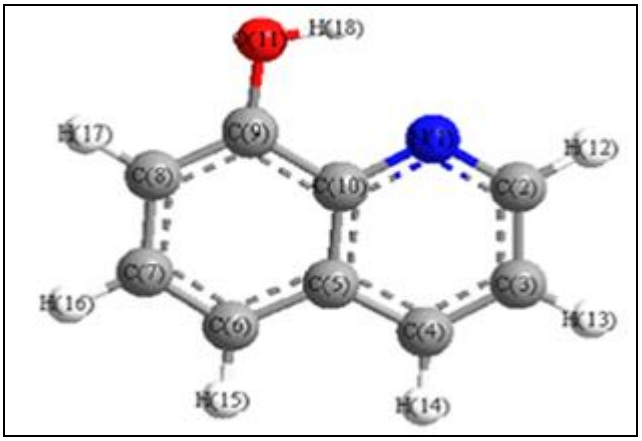


**FIG. 1: STRUCTURAL REPRESENTATION OF 8-HUDROXYQUINOLINE**

**TABLE 2: NATURAL BOND ORBITAL (NBO) ANALYSIS USING B3LYP/6-31G(d,P)**

| Donor(i) | Type | Acceptor (j) | Type | E(2)[a] | E(j)_E(i)[b] [a.u.] | F(i; j)[c] [a.u.] |
|---|---|---|---|---|---|---|
| C1 - C2 | π | C3 - C4 | π* | 17.81 | 0.28 | 0.067 |
| C1 - C2 | π | C5 - C6 | π * | 14.91 | 0.29 | 0.060 |
| C3 - C4 | π | C1 - C2 | π * | 14.81 | 0.28 | 0.060 |
| C3 - C4 | π | C5 - C6 | π * | 18.33 | 0.27 | 0.065 |
| C3 - C4 | π | C10 - C13 | π * | 17.28 | 0.27 | 0.065 |
| C3 - C4 | π | C12 - N18 | π * | 15.88 | 0.26 | 0.060 |
| C 5 - C6 | π | C1 - C2 | π * | 19.93 | 0.30 | 0.070 |
| C 5 - C6 | π | C3 - C4 | π * | 13.68 | 0.29 | 0.059 |
| C10 -C13 | π | C3 - C4 | π * | 15.21 | 0.29 | 0.063 |
| C10 -C13 | π | C12 -N18 | π * | 23.11 | 0.28 | 0.073 |
| C12 -N18 | π | C3 - C4 | π * | 19.34 | 0.33 | 0.076 |
| C12 -N18 | π | C10 - C13 | π * | 12.18 | 0.33 | 0.057 |
| O16 | LP(2) | C5 - C6 | π * | 32.52 | 0.35 | 0.099 |
| N18 | LP(1) | C3 - C4 | π * | 10.57 | 0.86 | 0.086 |
| N18 | LP(1) | C3 - C4 | π * | 2.20 | 0.85 | 0.039 |
| N18 | LP(1) | C4 - C5 | π * | 10.65 | 0.87 | 0.087 |

[a]$E^{(2)}$ means energy of hyper conjugative interaction (stabilization energyin kJ/mol).
[b]Energy difference between donor and acceptor i and j NBO orbitals.
[c]F(i; j) is the Fock matrix element between i and j NBO orbitals.

**TABLE 3: NATURAL BOND ORBITAL (NBO) ANALYSIS USING B3LYP/6-31G(d,P)**

| Donor(i) | Type | Acceptor (j) | Type | E(2)[a] | E(j)-E(i)[b] [a.u.] | F(i; j)[c] [a.u.] |
|---|---|---|---|---|---|---|
| C1 - C2 | π | C3 - C4 | π* | 23.29 | 0.36 | 0.087 |
| C1 - C2 | π | C5 - C6 | π * | 19.12 | 0.37 | 0.077 |
| C3 - C4 | π | C1 - C2 | π * | 18.80 | 0.36 | 0.077 |
| C3 - C4 | π | C5 - C6 | π * | 22.60 | 0.35 | 0.082 |
| C3 - C4 | π | C10 - C13 | π * | 22.67 | 0.35 | 0.084 |
| C3 - C4 | π | C12 - N18 | π * | 21.48 | 0.35 | 0.080 |
| C 5 - C6 | π | C1 - C2 | π * | 27.10 | 0.39 | 0.092 |

| | | | | | | |
|---|---|---|---|---|---|---|
| C 5 - C6 | π | C3 - C4 | π * | 18.06 | 0.37 | 0.076 |
| C10 - C13 | π | C3 - C4 | π * | 19.84 | 0.37 | 0.080 |
| C10 - C13 | π | C12 - N18 | π * | 29.97 | 0.37 | 0.095 |
| C12 - N18 | π | C3 - C4 | π * | 25.39 | 0.41 | 0.097 |
| C12 - N18 | π | C10 - C13 | π * | 16.10 | 0.42 | 0.074 |
| O16 | LP(2) | C5 - C6 | π * | 39.64 | 0.46 | 0.126 |
| N18 | LP | C3 - C4 | π * | 11.89 | 1.01 | 0.099 |
| N18 | LP | C12 – C13 | π * | 12.30 | 1.00 | 0.100 |

See **Table 2** foot note for the definition of superscripted alphabets ([a, b, c])

The stabilization energies vary among the different orbitals as exhibited in **Table 2** and **3**. Presented data in **Table 2** has determined using B3LYP/6-31G(d,P) level of theory. The high probable transition takes place in 8-HQ as (C10-C13)→ π*(C12-N18) with 23.11 kJ/mol. It is the enormous value among all the stabilization energies. Other transitions such as π(C12-C18)→ π*(C3-C4) and π (C3-C4)→ π*(C5-C6) also show a very high stabilization energies as 19.34 kJ/mol and 18.33 kJ/mol respectively. While transition as π(C12-N18)→π*(C10-C13) contains 12.18 kJ/mol. This is the least stabilization energy among all. This lowest energy results in the weak interaction between the electron donor and acceptor.

The same trend of interaction is also noticed in relation to resonance in the molecule. For example LP(O16)→ π*(C5-C6) produces 32.52 kJ/mol. This is the highest value. While LP(N18) → π*(C3-C4) produces 2.20 kJ/mol which exhibits a very low electron donating interaction energy.

Presented data in **Table 3** has been determined using M06-2X/6-31G(d,P) level of theory. The interaction as π(C10-C13)→π*(C12-N18) has the highest value (29.97 kJ/mol) among all the energies. Some other stabilization energies are 27.10 kJ/mol and 25.39 kJ/mol due to π(C5-C6)→ π*(C1-C2) and π(C12-C18)→ π*(C3-C4) respectively. These values also show the strong stabilization energies. However π (C12- C18)→ π*(C10-C13) and π(C5- C6) → π* (C3-C4) have the interaction energies 16.10kJ/mol and 18.06 kJ/mol respectively, which are the least values among the whole data of donor (π) and acceptor (π*). In case of the resonance, the transition as LP(O16)→ π*(C5-C6) has energy value 39.64 kJ/mol which is enormous energy value. While a least value 11.89 kJ/mol was exhibited by LP(N18)→ π*(C3-C4). By comparing the data of both **Tables 2** and **3**, it is concluded that the highest energy values are calculated at M06-2X/6-31G(d,P) as compared to B3LYP/6-31G(d,p) level.

For example, the highest stabilization energies such as 39.64 and 29.97 kJ/mol are represented at M06-2X/6-31G(d,P) level (**Table 3).** In contrast, the maximum stabilization energies are found to be 32.52 and 23.11 kJ/mol at the B3LYP/6-31G(d,p) level (**Table 2**).

Some conflicts are detected with the assignment of the C10 reported by R. P. Gangadharan et al. (2014) in which the C10 containing LP(1) with high stabilization energy as 81.91 kJ/mol was reported.7 In the recent study, same reported method as B3LYP/6-31G(d,p) and new M06-2X/6-31G(d,P) method are used to clear this confusion from the literature. Anyway, there is no carbon of the molecule showed any lone pair [LP(1)] see **Table 2** and **3**. As it is obvious that carbon never contains any lone pair [LP(1)] in neutral molecule. Moreover, in the present study, the maximum stabilization energies reached up to 32.52 and 39.64 kJ/mol due to lone pairs [LP(2)] of oxygen in B3LYP/6-31G(d,p) and M06-2X/6-31G(d,P) methods respectively. These energies are around about 2 times less than reported values. Although, the M06-2X level is considered most authentic method to calculate the non covalent interactions (NCIs), stabilization energy, high accuracy in thermochemistry and excitation electronic energies for valence and rydberg states. [21]

**FT-IR and FT-Raman analysis:** The quantity of atoms in 8-HQ are 48 atoms with symmetry point group C1. The active vibrational normal modes are also found to be 48 in FT-IR and FT-Raman spectra. The vibrational modes were assigned with the help of animation option of Avogadro software. The calculated frequencies are summarized in **Table 4**.

**TABLE 4: CALCULATED VIBRATIONAL FREQUENCIES OF 8-HQ BY M06-2X/6-31G(d,P)**

| [a]Freq | [a]$I_{IR}$ | [a]$I_{Raman}$ | Vibrational assignments |
|---|---|---|---|
| 416 | 80 | 5 | υ(τ)O-H |
| 443 | 30 | 3 | υ(γ)O-H+ υ( γ)C-$H_{Ben}$ |
| 474 | 0.56 | 7 | υ(δ) H-C=C-H |
| 478 | 0.86 | 0.28 | υ(τ)C-$H_{Ben}$ |
| 492 | 0.48 | 5 | υ( s) C-N=C-H |
| 549 | 5 | 3 | υ(δ) O-H + υ( δ) C-$H_{Ben}$ |
| 583 | 5 | 6 | υ(δ) C=C-C=N |
| 598 | 0.43 | 3 | υ(w) C-$H_{Ben}$ |
| 659 | 2.1 | 1.08 | υ(τ)C-$H_{Ben}$ |
| 729 | 6 | 27 | υ(s) C-C=C |
| 770 | 32 | 5 | υ(w) C-$H_{Ben}$ |
| 813 | 14 | 2.34 | υ(w) C-$H_{Ben}$ |
| 818 | 10 | 1.71 | υ(s) H-C=C-H |
| 839 | 53 | 0.04 | υ(w) C-$H_{Ben}$ |
| 890 | 0.01 | 4 | υ( τ)C-$H_{Ben}$ |
| 902 | 3.4 | 2 | υ(as) H-C=C-H |
| 978 | 0.29 | 4 | υ( τ)C-$H_{Ben}$ |
| 982 | 0.96 | 0.19 | υ( τ)C-$H_{Ben}$ |
| 1020 | 0.9 | 0.07 | υ(w) C-$H_{Ben}$ |
| 1060 | 6.8 | 5 | υ( τ)C-$H_{Ben}$+ υ(s) C-C |
| 1091 | 55 | 3 | υ( δ) C-$H_{Ben}$ |
| 1120 | 42 | 7 | υ( δ) C-$H_{Ben}$ |
| 1162 | 0.33 | 10 | υ( δ) C-$H_{Ben}$ |
| 1187 | 25 | 5 | υ( δ) C-$H_{Ben}$+ υ( ρ) O-H |
| 1227 | 21 | 2.28 | υ( ρ) C-$H_{Ben}$ |
| 1259 | 22 | 1.38 | υ( δ) C-$H_{Ben}$ |
| 1296 | 43 | 3 | υ(ρ) C-$H_{Ben}$ |
| 1326 | 21 | 5 | υ( ρ) C-$H_{Ben}$ |
| 1397 | 82 | 10 | υ( ρ) C-$H_{Ben}$+ υ( δ) O-H |
| 1434 | 44 | 64 | υ(s) C-$H_{Ben}$+ υ(s) C-C |
| 1453 | 4.6 | 35 | υ( ρ) C-$H_{Ben}$+ υ(s) C-C-N |
| 1486 | 40 | 132 | υ(s) C-$H_{Ben}$+ υ(s) C-C |
| 1541 | 16 | 4 | υ( ρ) C-$H_{Ben}$+ υ(as) C-C |
| 1590 | 78 | 0.25 | υ( ρ) C-HBen+ υ(s) O-H+ υ(s) C-C |
| 1671 | 39 | 40 | υ(s)C-C=C+βC-C=C |
| 1698 | 25 | 4 | υ(s)C-C=C+βC-C=C |
| 1721 | 20 | 3 | υ(as)C-C=C+βC-C=C |
| 3176 | 24 | 154 | υ(as) C-HBen |
| 3196 | 10 | 74 | υ(as) C-HBen |
| 3209 | 10 | 128 | υ(s) C-HBen+ υ(as)C-HBen |
| 3211 | 5.0 | 72 | υ(s) C-HBen |
| 3226 | 11 | 150 | υ(s) C-HBen |
| 3231 | 12 | 231 | υ(s) C-HBen |
| 3897 | 71 | 145 | υO-H |

Frequencies are given in $cm^{-1}$, υ =stretching, β =in-plane bending, γ=out-plane bending δ =scissoring, ρ =rocking, w= wagging, s =symmetric, as=asymmetric, τ =twisting, Ben=benzene ring.

**O-H vibrations:** The FT-IR and FT-Raman modes of hydroxyl group (OH) in 8-hydroxyquinoline have been located at 3418, 1456 and 896 $cm^{-1}$.**Error! Bookmark not defined.** In the current study, the vibrations of C-H and O-H are mostly observed at 443, 549, 1187 and 1397 $cm^{-1}$. The vibrational frequency for O-H is located at 3897$cm^{-1}$ and their assignments can be seen in **Table 4**.

**C-H stretching vibration:** The C-H vibrations of heteroaromatic organic compounds and their derivatives are found very close to C-H vibrations in benzene ring. They consist of multiple weak bands in range of 3100-3000 $cm^{-1}$ due to stretching vibrations of C-H. [22] In current study, the aromatic ring carbon-hydrogen (C-H) stretching frequencies occurred at a range 3231-3176 $cm^{-1}$ in FT-IR and FT-Raman.

However, the Raman intensities are found stronger than FT-IR intensities for above mentioned vibrational frequencies.

The assignments of mentioned vibrational frequencies are observed: the aromatic ring carbon-hydrogen (C-H) stretching showed symmetric modes at 3231 and 3226 $cm^{-1}$. While anti-symmetric stretching modes of C-H are observed at 3196 and 3176 $cm^{-1}$. However 3209 $cm^{-1}$ is the only frequency mode in this range which showed both symmetric and anti-symmetric stretching of C-H.

In hydroxyquinoline derivatives, C-H vibrations were also studied in range 1247-1087 $cm^{-1}$. **Error! Bookmark not defined.** In the current study, the C-H stretching modes and their intensities are also observed at low frequencies as shown in **Table 4**. The rocking stretching modes are found to be 1326, 1296 and 1227 $cm^{-1}$. While, the scissoring frequencies are ranged in 1162-1091 $cm^{-1}$. The wagging bands are observed at 1020, 839, 813, 770 and 598 $cm^{-1}$. The twisting vibrations of C-H are observed at 982, 978, 890, 659 and 478 $cm^{-1}$ as can be seen in **Table 4**.

**C-C stretching vibration:** The C-C stretching vibrations in the benzene derivatives appear in range of 1650-1400 $cm^{-1}$.[23] In this study, a similar trend of C-C vibrations is observed at 1721-1486 $cm^{-1}$ and their assignments can be seen in **Table 4**.

**C-N bands:** The evaluation of C-N bands is difficult task due to the possibility of overlapping with several other vibrations. The C-N stretching modes are observed at 1600, 1450, 1286 and 1273 $cm^{-1}$ as can be seen in **Table 4**. The FT-IR and Raman frequencies were calculated by using method B3LYP /6-31G(d) in gas and solvent phase. The results are tabulated in **Table 5.**

**TABLE 5: CALCULATED VIBRATIONAL FREQUENCIES USING B3LYP/6-31G(d) IN GAS AND SOLVENT PHASE**

| Gas Phase | | | | Solvent Phase[b] | | | |
|---|---|---|---|---|---|---|---|
| Frequency Unscaled | Frequency Scaled[a] | $I_{IR}$ | $I_{Raman}$ | Frequency Unscaled | Frequency Scaled[a] | $I_{IR}$ | $I_{Raman}$ |
| 137 | 132 | 0.8782 | 1.5121 | 134 | 129 | 2.7372 | 3.5805 |
| 177 | 170 | 6.5759 | 0.1195 | 176 | 169 | 9.4653 | 0.2082 |
| 267 | 257 | 4.1632 | 0.9354 | 263 | 253 | 11.7116 | 1.8121 |
| 286 | 275 | 7.8046 | 1.3711 | 288 | 277 | 13.0914 | 2.7918 |
| 405 | 389 | 88.6766 | 4.9427 | 378 | 363 | 135.1242 | 8.4871 |
| 440 | 423 | 16.9382 | 2.8406 | 436 | 419 | 6.9541 | 6.7659 |
| 470 | 453 | 0.5153 | 6.8084 | 469 | 451 | 1.032 | 14.0655 |
| 480 | 462 | 0.4826 | 0.3724 | 480 | 461 | 0.0051 | 0.4244 |
| 491 | 472 | 0.3334 | 5.0577 | 491 | 472 | 0.3685 | 12.7386 |
| 546 | 525 | 5.4075 | 4.0793 | 544 | 523 | 8.9243 | 8.7544 |
| 585 | 562 | 3.7901 | 7.3314 | 584 | 561 | 5.451 | 17.3027 |
| 593 | 570 | 0.206 | 2.5227 | 593 | 570 | 0.4699 | 4.1147 |
| 651 | 626 | 1.7612 | 0.8915 | 650 | 625 | 2.4071 | 1.1882 |
| 718 | 690. | 5.8373 | 30.4289 | 716 | 688 | 13.0399 | 77.2163 |
| 763 | 733 | 27.637 | 3.977 | 768 | 738 | 41.8657 | 3.9044 |
| 805 | 774 | 21.912 | 1.9765 | 804 | 773 | 20.9449 | 4.3067 |
| 819 | 787 | 10.7307 | 1.122 | 816 | 785 | 17.0746 | 3.3164 |
| 831 | 799 | 37.1822 | 0.391 | 834 | 801 | 60.1606 | 0.752 |
| 866 | 832 | 1.155 | 3.2693 | 878 | 845 | 0.3944 | 3.9965 |
| 898 | 863 | 4.5371 | 1.7607 | 897 | 863 | 8.9497 | 6.9381 |
| 960 | 923 | 0.3468 | 0.0223 | 969 | 932 | 0.7135 | 3.3205 |
| 964 | 927 | 0.1897 | 3.4266 | 974 | 936 | 0.2248 | 1.7089 |
| 995 | 956 | 0.8516 | 0.1491 | 1006 | 967 | 1.2269 | 0.5807 |
| 1058 | 1017 | 7.2201 | 6.6479 | 1059 | 1018 | 27.7016 | 16.1963 |
| 1084 | 1041 | 63.8909 | 4.624 | 1079 | 1038 | 104.9651 | 17.6372 |
| 1114 | 1071 | 34.8322 | 9.516 | 1110 | 1067 | 70.8533 | 30.9298 |
| 1169 | 1124 | 0.6704 | 8.1774 | 1168 | 1123 | 1.7045 | 19.0348 |
| 1197 | 1150.4 | 17.0417 | 1.9885 | 1193 | 1147 | 24.0337 | 1.7467 |
| 1230 | 1182 | 25.1357 | 2.9646 | 1229 | 1182 | 39.9485 | 8.6426 |
| 1259 | 1211 | 8.191 | 2.2252 | 1256 | 1208 | 8.4728 | 10.7766 |
| 1297 | 1247 | 52.724 | 4.2669 | 1293 | 1243 | 99.3074 | 8.396 |

| | | | | | | | |
|---|---|---|---|---|---|---|---|
| 1321 | 1270 | 29.2186 | 8.3763 | 1315 | 1264 | 46.4538 | 32.8852 |
| 1386 | 1333 | 80.9085 | 23.0063 | 1378 | 1324 | 143.7059 | 46.1463 |
| 1408 | 1353 | 55.2562 | 87.2255 | 1405 | 1355 | 79.1135 | 403.9155 |
| 1449 | 1393 | 0.2306 | 17.621 | 1447 | 1391 | 1.3109 | 58.2746 |
| 1480 | 1423 | 42.909 | 75.8039 | 1477 | 1420 | 67.847 | 219.1444 |
| 1525 | 1466 | 11.2768 | 5.2207 | 1521 | 1463 | 26.6199 | 13.8429 |
| 1566 | 1505 | 43.9668 | 0.2358 | 1563 | 1502 | 95.3223 | 1.3084 |
| 1624 | 1561 | 39.7479 | 40.1334 | 1620 | 1558 | 44.1799 | 155.3946 |
| 1657 | 1593 | 15.3705 | 6.2409 | 1653 | 1589 | 24.6183 | 20.3393 |
| 1674 | 1609 | 19.0884 | 2.198 | 1671 | 1607 | 25.656 | 4.665 |
| 3160 | 3038 | 31.4188 | 150.2075 | 3166 | 3042 | 56.8655 | 351.9797 |
| 3167 | 3044 | 20.1376 | 106.4854 | 3183 | 3060 | 20.4974 | 225.9812 |
| 3183 | 3060 | 5.7772 | 25.7498 | 3194 | 3070 | 2.6982 | 19.519 |
| 3187 | 3064 | 11.0221 | 106.0116 | 3196 | 3073 | 23.3264 | 309.8756 |
| 3206 | 3082 | 28.599 | 172.6484 | 3212 | 3088 | 38.5252 | 469.8366 |
| 3210 | 3086 | 22.2084 | 266.8348 | 3220 | 3096 | 29.8359 | 529.5724 |
| 3741 | 3596 | 44.098 | 154.9709 | 3729 | 3585 | 109.1334 | 310.4658 |

Frequency units are given in $cm^{-1}$, [a]scaling factor= 0.9613,[9] [b]solvent=DMSO.

According to this data the values of the FT- IR and Raman frequencies are increased in solvent phase than gas phase such as 288,768, 834, 878, 969, 974, 1006, 1059 and 3166-3220 $cm^{-1}$. While in gas phase frequencies like 137,177, 267, 405, 440, 470, 546, 585, 651,718, 805, 819, 898, 1084-1674 and 3741 are shifted upward as compared to solvent phase. Hence, the straightforward relation is not observed between solvent and gas phase.

However, a significant straightforward relation is observed in intensities of IR and Raman of both solvent and gas phase. The intensities of FT-IR and FT-Raman are remarkably increased in solvent than gas phase. For example the frequencies as 378, 716,1079,1378,1405, 3166, 3220 and 3790 $cm^{-1}$ showed the maximum intensities in solvent phase. In current study, a good agreement is observed in FT-IR and Raman frequencies computed by both M06-2X/6-31G (d,P) and B3LYP/6-31G (d,p) method. However, these vibrational frequencies are slightly greater than the reported frequencies. **Error! Bookmark not defined.**, **Error! Bookmark not defined.** The solute-solvent interactions can be well explained with the help of free energy difference.[24] The solvation free energy is calculated through PCM model [25] by pursuing electrostatic, dispersions, repulsions, and cavitations terms. These terms can be shown by following relationship.

$$G_{solvation} = G_{electrostatic} + G_{dispersion\text{-}repulsion} + G_{cavitation}$$

Nevertheless, in SMD (Density-based Solvation Model), [26] the process of solvation free energy is completely different than PCM model. This model involves complete solute electron density without considering partial atomic charges.

**TABLE 6: DIPOLE MOMENT, FREE ENERGY AND SOLVATION FREE ENERGY USING PCM AND SMD.**

| | Dipole Moment[a] | Free Energy [b] | Salvation Free Energy[b] |
|---|---|---|---|
| Gas Phase | 2.21 | -1252456 | |
| PCM model | 3.10 | -1252484 | -28.7 |
| SMD model | 3.21 | -1252495 | -39.5 |

[a] units in Debye, [b] units in kJ/mol

In the present study, the PCM and SMD models have been compared, and the calculated dipole moment solvation free energies are summarized in **Table 6.** The dipole moment and free energies are obtained to be greater in solution than the gas phase The dipole moment and solvation free energies are found to be 3.10 $\mu$ and -28.7 kJ/mol in PCM model. While, SMD model showed the dipole moment and solvation free energies are 3.21 $\mu$ and -39.5 kJ/mol. By comparing PCM and SMD models, the solvation free energy and dipole moment is increased in SMD model than PCM model.

**UV-Visible analysis:** The ultraviolet spectral analysis was calculated by M06-2X/6-31G(d,P) method. The outcomes of ultraviolet spectrum are represented in **Table 7.**

**TABLE 7: WAVE LENGTH, EXCITATION ENERGY, AND OSCILLATOR STRENGTH OF 8-HQ**

| λ (nm) | E (eV) | *f* | MO contributions |
|---|---|---|---|
| 273.97 | 4.5254 | 0.0028 | H-2 →L (90%), H-2 →L+2(6%) |
| 269.58 | 4.5991 | 0.0763 | H-1 →L+1(3%), H →L(96%) |
| 260.70 | 4.7559 | 0.0051 | H-1 →L (40%), H →L+1(57%) |
| 218.09 | 5.6851 | 0.0000 | H-2→L+1 (96%) |
| 207.53 | 5.9744 | 0.7542 | H-3 →L+1 (5%), H-1 → L(51%), H-1 → L+2(4%) H L+1 → (38%) |
| 191.64 | 6.4696 | 0.0416 | H-3 →L (15%), H-1 → L+1 (62%), H→ L+2 (20%) |

MO=molecular orbital, H=Homo, L=LUMO, ***f***= oscillator strength

**Table 7** shows the wavelengths as 191.67, 269.58 and 207.59 nm with oscillator strengths i.e 0.0763, 0.0416 and 0.7542 respectively which indicate relatively stronger allowed transitions. While the wavelengths as 260.70 and 269.58 nm with low magnitude of oscillator strength show weak transitions. Frontier molecular orbitals (FMOs). The frontier molecular orbital (FMOs) theory has been recognized as a most outstanding theory in elucidating the chemical stability of species. [27] The highest occupied molecular orbital is denoted by HOMO and lowest unoccupied molecular orbital is denoted by LUMO, which are considered substantial orbitals of frontier molecular orbitals (FMOs). Usually, the HOMO vitality demonstrates the capacity of donating an electron, though, the LUMO vitality speaks to the capacity of picking up an electron. [28, 29] The frontier orbital energy gap is a valuable parameter in order to get knowledge regarding the dynamic stability and chemical reactivity of species. [30]

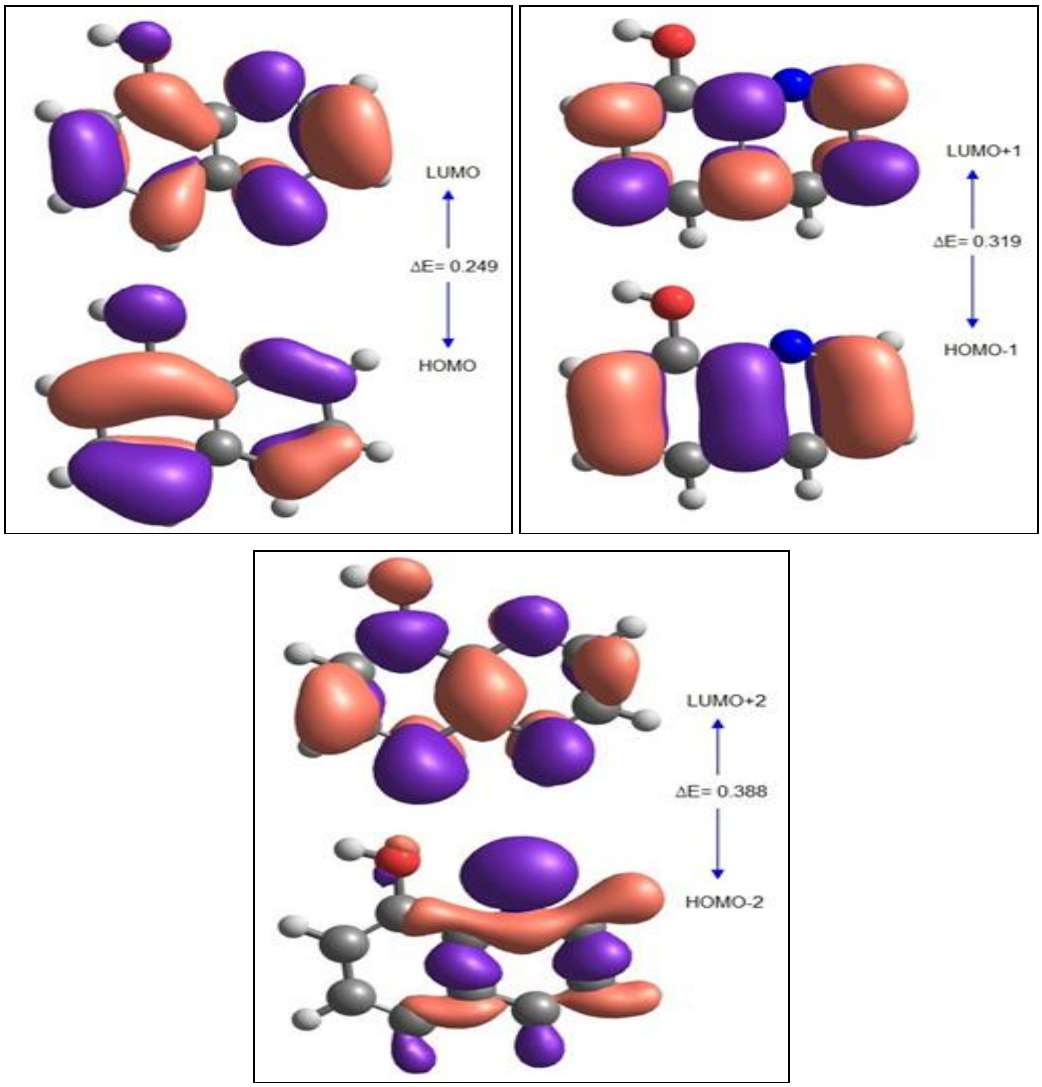


**FIG. 2: FRONTIER MOLECULAR ORBITALS OF 8-HQ AND UNITS IN HARTREE (a.u.).**

The orbital analysis of 8-HQ has been computed by using M06-2X/6-31G(d,p) method. The calculated energy of HOMO, LUMO, HOMO-1, LUMO+1, HOMO-2, LUMO+2 has been obtained around -0.2596, -0.0106, -0.2999, 0.0189, -0.314 and 0.074 a.u respectively. Subsequently, the energy gap such as $E_{HOMO}$–$E_{LUMO}$, $E_{HOMO-1}$–$E_{LUMO+1}$, $E_{HOMO-2}$–$E_{LUMO+2}$ were obtained 0.249, 0.319 and 0.388 respectively, see **Fig. 2**. The energies of FMOs are helpful to determine the global reactivity descriptors, such as global softness (*S*), electron affinity (*EA*), ionization potential (*IP*) [31], electro negativity (*X*) [32], global hardness ($\eta$), global electrophilicity index ($\omega$) and the chemical potential ($\mu$) u33-36 calculated utilizing Equations 2-8.

$$IP = -E_{HOMO} \quad \text{Equations 2}$$

$$EA = -E_{LUMO} \quad \text{Equations 3}$$

Where; IP defines Ionization potential (a.u), EA defines electron affinity (a.u).

The chemical potential (μ), electro negativity (X) and chemical hardness has been determined by using Koopmans's theorem [28] and as following Equations.

$$X = \frac{[IP + EA]}{2} = -\frac{[E_{LUMO} + E_{HOMO}]}{2} \quad \text{Equations 4}$$

$$\eta = \frac{[IP - EA]}{2} = -\frac{[E_{LUMO} - E_{HOMO}]}{2} \quad \text{Equations 5}$$

$$\mu = \frac{E_{HOMO}+E_{LUMO}}{2} \quad \text{Equations 6}$$

The global softness (σ) is defined by Equations 7 [37]

$$\sigma = \frac{1}{2\eta} \quad \text{Equations 7}$$

Parr et al. [38] introduced an electrophilicity index ($\omega$) and it can be described Equations 8.

$$\omega = \frac{\mu^2}{2\eta} \quad \text{Equations 8}$$

This parameter was proposed to describe the range of the electrophilic strength for specie

**TABLE 8: IONIZATION POTENTIAL (*IP*), ELECTRON AFFINITY(*EA*), ELECTRO NEGATIVITY (*X*) CHEMICAL POTENTIAL ($\mu$) GLOBAL HARDNESS ($\eta$) GLOBAL SOFTNESS (*S*) AND GLOBAL ELECTROPHILICITY ($\omega$).**

| | A | B | C |
|---|---|---|---|
| *IP* | -0.260 | -0.299 | -0.314 |
| *EA* | -0.011 | 0.019 | 0.074 |
| *X* | 0.135 | 0.141 | 0.120 |
| $\mu$ | -0.135 | -0.141 | -0.120 |
| $\eta$ | 0.249 | 0.319 | 0.388 |
| *S* | 4.016 | 3.137 | 2.577 |
| $\omega$ | 0.073 | 0.062 | 0.037 |

A= HOMO & LUMO, B= HOMO-1 & LUMO+1, C= HOMO-2 & LUMO+2, units in Hartree ($E_h$).

The stability, selectivity and reactivity of specie can be described by global reactivity parameters. [39-42] The most important chemical property is electronegativity which described the capacity of specie to attract electrons towards itself. The global softness (S) of this molecule is found to be 4.016 Eh. It is 16 times greater than the magnitude of global hardness (η). These findings suggest that this molecule contain less hardness and larger softness values because of the low HOMO–LUMO energy gap. The softness value reveals that the molecule may be biological activate. This indication has good agreement to reported biological activities of 8-HQ.

**Molecular electrostatic potential (MEP):** The three dimensional plot of total electron density is known as molecular electrostatic potential (MEP). MEP surface is developed utilizing the optimized geometry of title compound at the M06-2X/6-31G(d,p) level of theory. MEP can be significant descriptor for explanation of non-covalent interactions (NCIs), attack of electrophilic and nucleophilic at appropriate zone of investigated system. [43] The magnitude of electrostatic potential at the MEP map are addressed by standard colors i.e. red color defines the most negative zones, blue displays the most positive and green assume the role of the zero electrostatic potential, therefore, the charge contribution can be ordered i.e. red > orange > yellow >green > blue. Accordingly, the negative (red and yellow) zones on MEP have been associated to the chance of electrophilic attack and the positive zones (blue) to encounter nucleophilic.

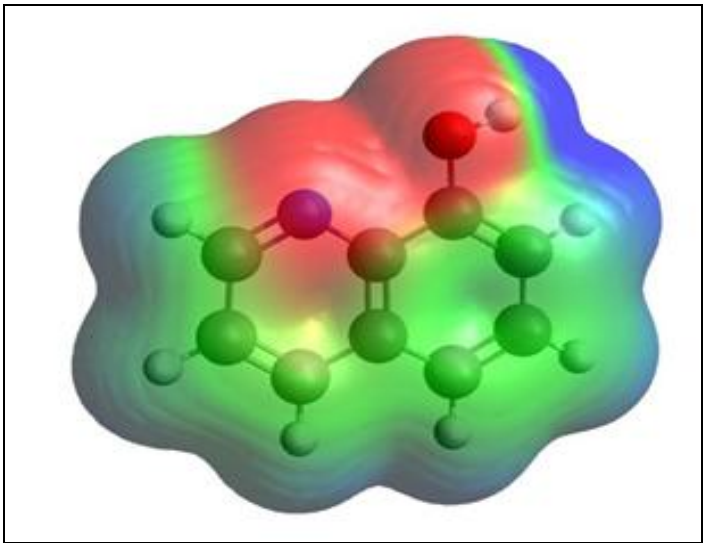

**FIG. 3: MOLECULAR ELECTROSTATIC POTENTIAL MAP FOR TITLE COMPOUND**

**Fig. 3** shows, negative potential which is confined over the oxygen atoms and the N atoms, whereas positive region is confined around the hydrogen atoms.

**Thermodynamic parameters:** The thermodynamics parameters of 8-HQ were calculated using the M06-2X/6-31G(d,p) and B3LYP/6-31G(d) methods and presented in **Table 9**.

**TABLE 9: THERMODYNAMIC PARAMETERS OF 8-HQ WITH VARIOUS TEMPERATURES**

| T (K) | $S_m^0$ (J/mol.K)[a] | $C_{p,m}^0$ (J/mol.K)[a] | $H_m^0$ (kJ/mol)[a] | $S_m^0$ (J/mol.K)[b] | $C_{p,m}^0$ (J/mol.K)[b] | $H_m^0$ (kJ/mol)[b] |
|---|---|---|---|---|---|---|
| 25.00 | 212.50 | 33.55 | 0.83 | 212.59 | 33.54 | 0.83 |
| 100.00 | 267.97 | 54.26 | 4.01 | 267.95 | 54.08 | 4.00 |
| 200.00 | 318.92 | 100.11 | 11.62 | 318.63 | 99.47 | 11.57 |
| 298.15 | 368.27 | 150.34 | 23.92 | 367.67 | 149.39 | 23.79 |
| 300.00 | 369.21 | 151.27 | 24.19 | 368.60 | 150.32 | 24.07 |
| 400.00 | 419.27 | 197.76 | 41.71 | 418.37 | 196.72 | 41.48 |
| 500.00 | 467.65 | 235.81 | 63.46 | 466.52 | 234.82 | 63.13 |
| 600.00 | 513.41 | 265.87 | 88.60 | 512.11 | 264.99 | 88.18 |
| 700.00 | 556.25 | 289.72 | 116.43 | 554.82 | 288.93 | 115.92 |
| 800.00 | 596.24 | 308.95 | 146.39 | 594.71 | 308.25 | 145.81 |
| 900.00 | 633.57 | 324.72 | 178.10 | 631.96 | 324.10 | 177.45 |
| 1000.0 | 668.48 | 337.85 | 211.25 | 666.81 | 337.30 | 210.54 |

[a]Calculated via M06-2X/6-31G(d,p),[b]Calculated via B3LYP/6-31G(d).

The thermodynamics parameters calculated by two methods namely M06-2X and B3LYP with same basis set as 6-31G (d). The magnitude of thermodynamics parameters is appeared to be similar in both methods. The rise in temperature (25-1000K) enhanced the molecular vibration which in turn increases the entropy (*S*), heat capacity (*C*) and enthalpy (*H*).

**CONCLUSION:** The present study indicates that the optimized bond lengths and bond angles show good correspondence with the reported X-ray and DFT based data. As reported in literature that the C10 contain LP(1) with high stabilization energy as 81.91 kJ/mol. However, the findings of both B3LYP/6-31G(d,p) and M06-2X/6-31G(d,P) methods indicated that there is no lone pair on carbon of the title compound. It is obvious that carbon never contains any lone pair in neutral molecule. The maximum stabilization energy reached up to 39.64kJ/mol which is 2 times less than reported value. The FT- IR and Raman frequencies have increased as compared to reported values in all methods, but good consistency is found from among investigated methods. In solvated 8-HQ, the FT- IR and Raman frequencies are almost insensitive to medium effects.

However, significant medium effect on FT-IR and FT-Raman intensities is observed. The intensities enhanced from gas to solvent phase. The dipole moments are found to be 3.10 and 3.21 and solvation free energies are -28.710 and -39.456 kJ/mol in PCM and SMD models respectively. By comparing both models, the dipole moment and solvation free energy are increased in SMD model than PCM model. FMOs suggest that this molecule contain less hardness and larger softness values. These findings reveal that the molecule might be bioactive.

**ACKNOWLEDGMENTS:** The authors are grateful to Sumaira Khalid for her valuable suggestions as well as a care full reading. Authors like to acknowledge Higher Education Commission (HEC) Pakistan. We also acknowledge Dr. Ana Paula L. Batista for her cooperation.

**DECLARATION OF INTEREST:** No conflicts declared.

## REFERENCES:

1. Martins, P, Jesus, J, Santos, S, Raposo, LR, Roma-Rodrigues, C, Baptista, PV and Fernandes, AR: Heterocyclic anticancer compounds: Recent advances and the paradigm shift towards the use of nanomedicine's tool box. Molecules 2015; 20:16852-16891.
2. Prachayasittikul, V, Prachayasittikul, S, Ruchirawat, S and Prachayasittikul, V: 8-hydroxyquinolines: A review of their metal chelating properties and medicinal applications. Drug design, development and therapy 2013; 7:1157.
3. Suwanjang, W, Prachayasittikul, S and Prachayasittikul, V: Effect of 8-hydroxyquinoline and derivatives on human neuroblastoma sh-sy5y cells under high glucose. PeerJ 2016; 4:e2389.
4. Patel, YS: Studies on metal complexes of 2-((8-hydroxyquinolin-5-yl) methylene) benzo [b] thiophen-3 (2h)-one 1, 1-dioxide. Research on Chemical Intermediates 2015; 41:6611-6623.
5. Deshmukh, N, Das, PK and Karma, K: Synthesis and microbiological activity of 8-hydroxy quinoline derivatives and related compounds. Pharmaceutical and Biological Evaluations 2016; 3:135-139.
6. Serrao, E, Debnath, B, Otake, H, Kuang, Y, Christ, F, Debyser, Z and Neamati, N: Fragment-based discovery of 8-hydroxyquinoline inhibitors of the hiv-1 integrase–lens epithelium-derived growth factor/p75 (in–ledgf/p75) interaction. Journal of medicinal chemistry 2013; 56:2311-2322.
7. Al-Busafi, SN, Suliman, FEO and Al-Alawi, ZR: 8-hydroxyquinoline and its derivatives: Synthesis and applications. ChemInform 2014;45.
8. Arıcı, K, Yurdakul, M and Yurdakul, Ş: Hf and dft studies of the structure and vibrational spectra of 8-hydroxyquinoline and its mercury (ii) halide complexes. Spectrochimica Acta Part A: Molecular and Biomolecular Spectroscopy 2005; 61:37-43.
9. Krishnakumar, V and Ramasamy, R: Dft studies and vibrational spectra of isoquinoline and 8-hydroxyquinoline. Spectrochimica Acta Part A: Molecular and Biomolecular Spectroscopy 2005; 61:673-683.
10. Gangadharan, RP and Krishnan, SS: Natural bond orbital (nbo) population analysis of 1-azanapthalene-8-ol. Acta Physica Polonica A 2014; 125:18-22.
11. Halim, MA, Shaw, DM and Poirier, RA: Medium effect on the equilibrium geometries, vibrational frequencies and solvation energies of sulfanilamide. Journal of Molecular Structure: THEOCHEM 2010; 960:63-72.
12. Frisch, MJ, Trucks, GW, Schlegel, HB, Scuseria, G, Robb, MA, Cheeseman, JR, Scalmani, G, Barone, V, Mennucci, B, Petersson, G, Nakatsuji, H, Caricato, M, Li, X, Hratchian, HP, Izmaylov, AF, Bloino, J, Zheng, G, Sonnenberg, JL, Hada, M, Ehara, M, Toyota, K, Fukuda, R, Hasegawa, J, Ishida, M, Nakajima, T, Honda, Y, Kitao, O, Nakai, H, Vreven, T, Montgomery, JA, Peralta, JE, Ogliaro, F, Bearpark, M, Heyd, JJ, E, B, Kudin, KN, Staroverov, VN, Kobayashi, R, Normand, J, Raghavachari, K, Rendell, A, Burant, JC, Iyengar, SS, Tomasi, J, Cossi, M, Rega, N, Millam, JM, Klene, M, Knox, JE, Cross, JB, Bakken, V, Adamo, C, Jaramillo, J, Gomperts, R, Stratmann, RE, Yazyev, O, Austin, AJ, Cammi, R, Pomelli, C, Ochterski, JW, Martin, RL, Morokuma, K, Zakrzewski, VJ, Voth, GA, Salvador, P, Dannenberg, JJ, Dapprich, S, Daniels, AD, Farkas, O, Foresman, JB, Ortiz, JV, Cioslowski, J and Fox, DJ: D. 0109, revision d. 01, gaussian. Inc, Wallingford, CT 2009.
13. Kohn, W and Sham, LJ: Self-consistent equations including exchange and correlation effects. Physical review 1965; 140:A1133.
14. P, H and W, K: Inhomogeneous electron gas. Physical Review Letters 1964; 136:864-871.
15. Parr, RG and Weitao, Y. Oxford University Press, 1994.
16. Frisch, A, Nielsen, A and Holder, A: Gaussview users manual. Gaussian Inc, Pittsburgh, PA 2000.
17. Chemcraft. http:// www chemcraftprog com.
18. Avagadro. http://avogadrocc/wiki/Main_Page.
19. Banerjee, T and Saha, N: Hydrogen-bonding patterns in 8-hydroxyquinoline derivatives :(i) structure of 5-chloro-8-hydroxyquinoline and (ii) refinement of the structure of 8-hydroxyquinoline. Acta Crystallographica Section C: Crystal Structure Communications 1986; 42:1408-1411.
20. Khalid, M, Mashhadi, SMA, Imran, M, Yunus, U, Aslam, M and Bhatti, MH: International Journal of Agriculture & Applied Sciences 2016 :(in Press).
21. Gao, T, Li, H, Li, W, Li, L, Fang, C, Li, H, Hu, L, Lu, Y and Su, Z-M: A machine learning correction for dft non-covalent interactions based on the s22, s66 and x40 benchmark databases. Journal of cheminformatics 2016;8:1.
22. Chithambarathanu, T and Magdaline, JD: Vibrational spectroscopic investigations, conformational study, natural bond orbital and homo-lumo analysis of 2-benzoyl thiophene. Asian Journal of Chemistry 2015;27:4600.
23. Bellamy, L: The infra-red spectra of complex molecules. Springer Science & Business Media, 2013.
24. Madeira, PP, Bessa, A, Loureiro, JA, Álvares-Ribeiro, L, Rodrigues, AE and Zaslavsky, BY: Cooperativity between various types of polar solute–solvent interactions in aqueous media. Journal of Chromatography A 2015; 1408:108-117.
25. Ho, J and Ertem, MZ: Calculating free energy changes in continuum solvation models. The Journal of Physical Chemistry B 2016; 120:1319-1329.

26. Sundararaman, R and Goddard III, WA: The charge-asymmetric nonlocally determined local-electric (candle) solvation model. The Journal of Chemical Physics 2015; 142:064107.
27. Sebastian, S, Sylvestre, S, Jayabharathi, J, Ayyapan, S, Amalanathan, M, Oudayakumar, K and Herman, IA: Study on conformational stability, molecular structure, vibrational spectra, nbo, td-dft, homo and lumo analysis of 3, 5-dinitrosalicylic acid by dft techniques. Spectrochimica Acta Part A: Molecular and Biomolecular Spectroscopy 2015; 136:1107-1118.
28. Sun, LL, Zhang, T, Wang, J, Li, H, Yan, LK and Su, ZM: Exploring the influence of electron donating/withdrawing groups on hexamolybdate-based derivatives for efficient p-type dye-sensitized solar cells (dsscs). RSC Advances 2015; 5:39821-39827.
29. Amiri, SS, Makarem, S, Ahmar, H and Ashenagar, S: Theoretical studies and spectroscopic characterization of novel 4-methyl-5-((5-phenyl-1, 3, 4-oxadiazol-2-yl) thio) benzene-1, 2-diol. Journal of Molecular Structure 2016;1119:18-24.
30. Jeyavijayan, S: Molecular structure, spectroscopic (ftir, ft-raman, 13 c and 1 h nmr, uv), polarizability and first-order hyperpolarizability, homo–lumo analysis of 2, 4-difluoroacetophenone. Spectrochimica Acta Part A: Molecular and Biomolecular Spectroscopy 2015;136:553-566.
31. Fukui, K: Role of frontier orbitals in chemical reactions. Science 1982; 218:747–754.
32. Koopmans, T: Ordering of wave functions and eigenenergies to the individual electrons of an atom. Physica 1933; 1:104-113.
33. Lesar, A and Milošev, I: Density functional study of the corrosion inhibition properties of 1, 2, 4-triazole and its amino derivatives. Chemical physics letters 2009; 483:198-203.
34. Parr, RG, Donnelly, RA, Levy, M and Palke, WE: Electronegativity: The density functional viewpoint. The Journal of Chemical Physics 1978; 68:3801-3807.
35. Parr, RG, Szentpaly, Lv and Liu, S: Electrophilicity index. Journal of the American Chemical Society 1999; 121:1922-1924.
36. Sheela, N, Muthu, S and Sampathkrishnan, S: Molecular orbital studies (hardness, chemical potential and electrophilicity), vibrational investigation and theoretical nbo analysis of 4-4′-(1h-1, 2, 4-triazol-1-yl methylene) dibenzonitrile based on abinitio and dft methods. Spectrochimica Acta Part A: Molecular and Biomolecular Spectroscopy 2014;120:237-251.
37. Mahmood, A, Akram, T and de Lima, EB: Syntheses, spectroscopic investigation and electronic properties of two sulfonamide derivatives: A combined experimental and quantum chemical approach. Journal of Molecular Structure 2016;1108:496-507.
38. Parthasarathi, R, Padmanabhan, J, Elango, M, Subramanian, V and Chattaraj, P: Intermolecular reactivity through the generalized philicity concept. Chemical physics letters 2004;394:225-230.
39. Pratihar, S and Roy, S: Reactivity and selectivity of organotin reagents in allylation and arylation: Nucleophilicity parameter as a guide. Organometallics 2011; 30:3257-3269.
40. Heredia, C, Ferraresi-Curotto, V and López, M: Characterization of ptn (n= 2–12) clusters through global reactivity descriptors and vibrational spectroscopy, a theoretical study. Computational Materials Science 2012;53:18-24.
41. Mahmood, A, Khan, IU, Longo, RL, Irfan, A and Shahzad, SA: Synthesis and structure of 1-benzyl-5-amino-1h-tetrazole in the solid state and in solution: Combining x-ray diffraction, 1 h NMR, FT–IR, and UV–VIS spectra and DFT calculations. Comptes Rendus Chimie 2015;18:422-429.
42. Chattaraj, PK, Das, R, Duley, S and Vigneresse, J-L: Structure-stability diagrams and stability-reactivity landscapes: A conceptual dft study. Theoretical Chemistry Accounts 2012; 131:1-8.
43. Ríos-Gutiérrez, M, Domingo, LR and Pérez, P: Understanding the high reactivity of carbonyl compounds towards nucleophilic carbenoid intermediates generated from carbene isocyanides. RSC Advances 2015; 5:84797-84809.


**How to cite this article:**
Khalid M, Ali M, Aslam M, Sumrra SH, Khan MU, Raza N, Kumar N and Imran M: Frontier molecular, natural bond orbital, UV-Vis spectral study, solvent influence on geometric parameters, vibrational frequencies and solvation energies of 8-hydroxyquinoline. Int J Pharm Sci Res 2017; 8(2): 457-69.doi: 10.13040/IJPSR.0975-8232.8(2).457-69.